REVISTA DE LA
ASOCIACIÓN GEOLÓGICA ARGENTINA
www.geologica.org.ar
Julio 2025

Facies and depositional environment analysis of the southern sector of the Salar de Pocitos, Salta, Argentina

Laura Emilia GIMÉNEZ[1], Juan Ramiro LEZAMA[1,2], Claudia Inés GALLI[3], Eleonora ERDMANN[1,2]

[1]Instituto de Investigaciones para la Industria Química (INIQUI, CONICET-UNSa), Universidad Nacional de Salta, Av. Bolivia 5150, Salta, Argentina. (gimenezlaura60@gmail.com)

[2]Facultad de Ingeniería, Universidad Nacional de Salta, Av. Bolivia 5150, Salta, Argentina.

[3]Centro de Estudios Geológicos Andinos (CEGA-INSUGEO, CONICET-UNSa), Facultad de Ciencias Naturales, UNSa, Av. Bolivia 5150, Salta, Argentina.

Editor: Ricardo A. Astini

Recibido: 08/08/2024
Aceptado: 29/05/2025

ABSTRACT

Located in the Southern Puna, the Salar de Pocitos is a north–south trending endorheic basin covering an area of 405 km². The southern sector of the basin is bounded by the Coquena and Tolillar Formations, the Ojo de Colorados Basic Complex, and the Pastos Grandes Group. This portion of the basin hosts clastic and evaporitic deposits that act as reservoirs for lithium-enriched brines. This study aims to provide a sedimentological characterization of the basin fill in order to interpret the stratigraphic framework, depositional environments, and sedimentary evolution of the southern sector of the salar. Sedimentological analysis was based on core samples from four drillholes. Thirteen sedimentary facies were identified, additionally enabling a provenance study of the sandstones. Selley-style stratigraphic columns were constructed to facilitate facies correlation and the interpretation of depositional environments. In the southwestern area, fine-grained sandstones interbedded with claystones, carbonates, and halite dominate, whereas in the southeast, breccias, sandstones, siltstones, and crystalline halites are more prevalent. Toward the depocenter of the southern sector, fine-grained sandstones, breccias, siltstones, carbonates, and gypsum crystals associated with halite are common, while in the northern part of the study area, the deposits include thick beds of fine- to coarse-grained sandstones and halite, interbedded with claystones and siltstones. Sulfate minerals frequently cap the succession. The results suggest deposition within a playa-lake system, including alluvial fans, ephemeral fluvial systems, and shallow saline lakes—characteristic of endorheic basins in arid settings.

Keywords: evaporitic basin, sandstone provenance, playa lake.

RESUMEN

Análisis de facies y ambientes deposicionales del sector sur del Salar de Pocitos, Salta, Argentina
Ubicado en la Puna Sur, el Salar de Pocitos es una cuenca endorreica con una orientación norte–sur que abarca una superficie de 405 km². El sector sur de la cuenca está limitado por las Formaciones Coquena y Tolillar, el Complejo Básico Ojo de Colorados y el Grupo Pastos Grandes. Esta porción de la cuenca alberga depósitos clásticos y evaporíticos que actúan como reservorios de salmueras enriquecidas en litio. Este estudio tiene como objetivo realizar una caracterización sedimentológica del relleno de la cuenca para interpretar el marco estratigráfico, los ambientes deposicionales y la evolución sedimentaria del sector sur del salar. El análisis sedimentológico se basó en muestras de testigos corona provenientes de cuatro perforaciones. Se identificaron trece facies sedimentarias, lo que además permitió llevar a cabo un estudio de procedencia de las areniscas. Se construyeron columnas estratigráficas tipo Selley para facilitar la correlación de facies y la interpretación de los ambientes deposicionales. En el área suroeste predominan areniscas de grano fino intercaladas con arcilitas, carbonatos y halita, mientras que en el sureste son más frecuentes las brechas, areniscas, limolitas y halitas cristalinas. Hacia el depocentro del sector sur, son comunes las areniscas de grano fino, brechas, limolitas, carbonatos y cristales de yeso asociados con halita, mientras que, en la parte norte del área de estudio, los depósitos incluyen bancos gruesos de areniscas de grano fino a grueso y halita, intercalados con arcilitas y limolitas. Con frecuencia, la sucesión está coronada por minerales sulfatados. Los resultados sugieren una sedimentación dentro de un sistema de playa lake, que incluye

abanicos aluviales, sistemas fluviales efímeros y lagos salinos someros, característicos de cuencas endorreicas en ambientes áridos.

Palabras clave: cuenca evaporítica, procedencia de areniscas, *playa lake*.

INTRODUCTION

The Argentine Puna is a high-altitude plateau characterized by extensive endorheic depressions, known as salars. These depressions are bounded by mountain ranges of southern to submeridional orientation and by transverse volcanic chains aligned perpendicularly to the Andean trend (Turner and Méndez 1979, Sánchez et al. 2003). These geographical and geological features make the Puna a region of significant interest for sedimentological and paleoenvironmental studies. Within this vast plateau, the evaporitic basin of the Salar de Pocitos stretches between latitudes 24º 15' S and 24º 45' S and longitudes 66º 30' W and 67º 30' W, at an elevation of 3,700 meters above sea level. The Salar de Pocitos is located approximately 100 km west of San Antonio de los Cobres, the largest town on the Argentine altiplano, and roughly 250 km west of the provincial capital, Salta (Fig. 1).

The southern sector of the present Pocitos basin features a variety of clastic deposits, including breccias, sandstones, and shales, as well as evaporitic deposits such as halite and sulfates. These deposits serve as reservoirs for lithium-enriched brines. In salars where the concentration of sulfates, such as mirabilite and gypsum, increases, the presence of borates tends to decrease, often disappearing entirely. Borates (like colemanite, ulexite, or borax) tend to precipitate in alkaline, low-sulfate brines, especially rich in sodium and boron, whereas sulfates (like gypsum or mirabilite) tend to dominate in more saline, sulfate-rich, and often less alkaline environments. Thus, sulfate concentrations increase, the ionic composition of the brines shifting toward conditions that do not favor the stability or precipitation of borate minerals (Hardie et al. 1978, Warren 2016).

Such pattern can be observed in the Salar de Pocitos (Alonso 2006). The association of alluvial fan deposits with ephemeral stream sediments, aeolian sediments, red beds,

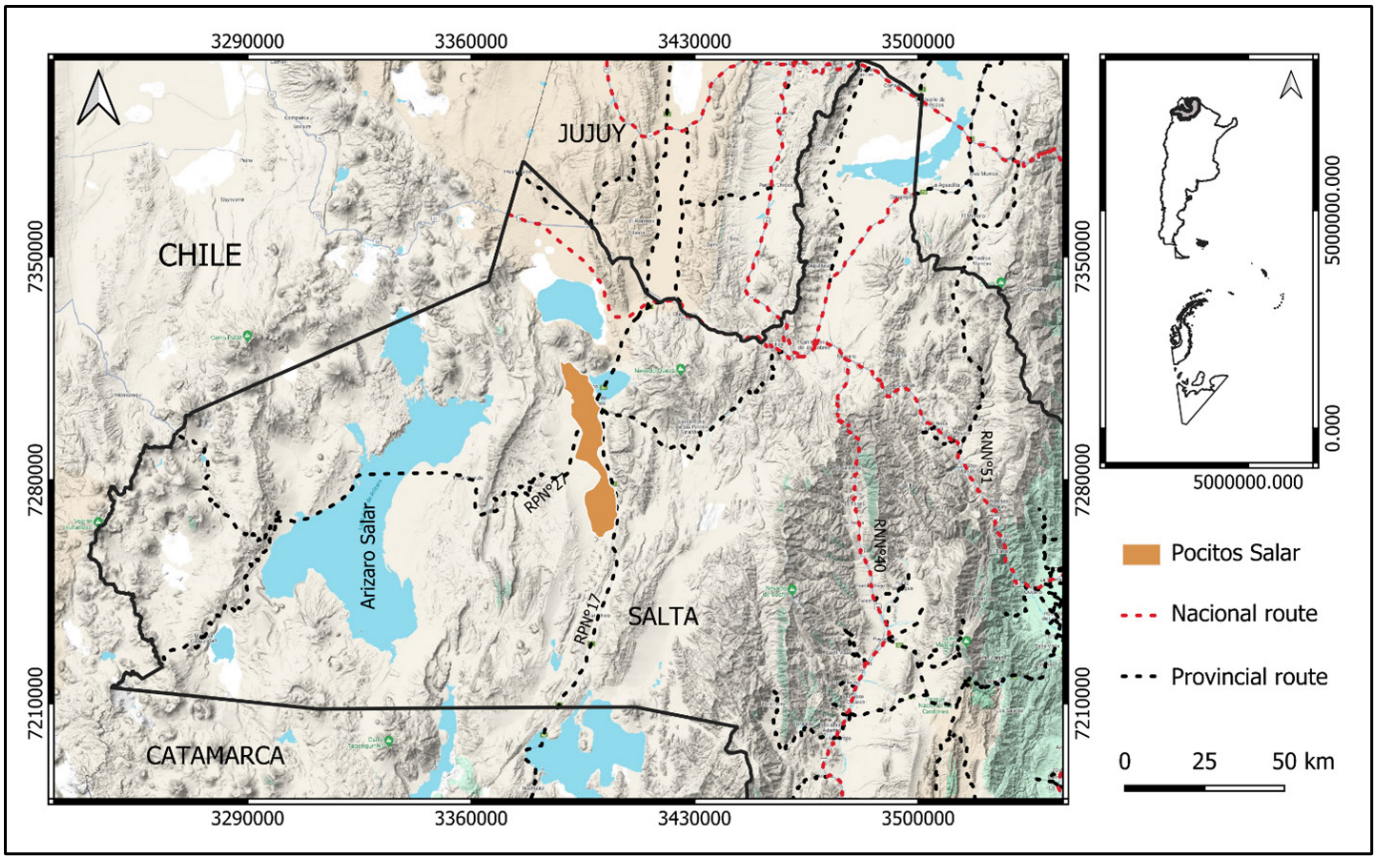

Figure 1. Location map of the Salar de Pocitos. EPSG:5345

and lacustrine carbonates suggests a non-marine origin for this basin.

An analysis of both ancient and modern evaporitic environments reveals alternating arid and humid conditions within this system (Alonso 2006). In this context, we propose that climate, in conjunction with tectonic activity, has played a key role in controlling sedimentation patterns, paleoenvironmental evolution, and the distribution of evaporite facies in the region.

Previous studies of the Salar de Pocitos have primarily focused on the compositional characteristics of evaporitic facies and travertines, providing valuable insights into regional geological processes. However, there has been no detailed attempt to correlate facies laterally, conduct a comprehensive provenance analysis of sandstones, or establish a precise framework for interpreting depositional environments within the basin. The significance and originality of this work lie in addressing these critical gaps in knowledge.

The objective of this study is to characterize the clastic and evaporitic sedimentary facies accumulated in the salar, define the associated depositional environments, and reconstruct the sedimentological evolution of the basin, particularly in its southern sector. In doing so, this research not only enhances our geological understanding of the region but also contributes valuable information for the exploration and sustainable development of mineral resources, with a focus on lithium-bearing brines.

GEOLOGICAL FRAMEWORK

The Salar de Pocitos is located in the geological province of the Puna, specifically within the southern Puna subprovince (Alonso et al. 1984). The structural features of the Neoproterozoic-Lower Paleozoic basement in the Puna have exerted varying influences on the subsequent development of both extensional structures during the Cretaceous and contractional structures in the Cenozoic (Hongn et al. 2010). The tectonic inversion of normal faults associated with Cretaceous rifting played a key role in the formation of Cretaceous normal faults that later underwent Cenozoic tectonic inversion, as well as in the development of Cenozoic reverse faults. Additionally, Hongn et al. (2010) suggested that the irregular temporal distribution of Andean shortening reflects the reactivation or inversion of structures, many of which exhibit superimposed movements from the Cretaceous to the Quaternary.

The current morphostructure of the Salar de Pocitos is the result of deformation processes younger than the lower Miocene, as indicated by the distribution of Eocene-Miocene sequences (Jordan and Mpodozis 2006). These tectonic processes, along with climatic conditions, have shaped the basin and significantly influenced the sedimentation and paleoenvironmental evolution of the region.

The Salar de Pocitos covers an area of approximately 405 km² and exhibits an elongated north–south geometry. A distinct narrowing occurs in its central section due to the development of alluvial fan deposits sourced from the surrounding mountain ranges to the east and west (Battaglia et al. 2001). The salar's eastern and western margins display contrasting morphologies. On the western flank, the boundary between the clastic alluvial fan facies and the evaporitic facies is sharp and well-defined. Alluvial deposits here form terrace levels, reflecting the gradual progradation of the saline body. In contrast, the eastern margin features a more diffuse transition between distal piedmont accumulations from the Cordón de Pozuelos and the expanding and retreating evaporitic deposits. Along this margin, remnants of silty–sandy lacustrine deposits with sparse gypsum and gypsarenite intercalations are preserved, attributed to a brief humid climatic pulse that interrupted prevailing Holocene aridity (Igarzábal 1996, Battaglia et al. 2001).

The southern sector of the basin spans 153 km². It is bounded by the Coquena Formation to the east, the Tolillar Formation and the Ojo de Colorados Basic Complex (Cerro Colorado Chico) to the south, and by the Cordón de Colorados to the west. The latter comprises exposures of the Gestes, Pozuelos, and Sijes formations, as well as Holocene alluvial terraces (Fig. 2). The Ordovician Coquena Formation consists primarily of fine-grained metasedimentary rocks of greenschist facies, including greywackes, quartzites, and phyllites. In areas of lower metamorphic grade, quartzitic sandstones and shales are also present (Turner 1960, Blasco et al. 1996). The Tolillar Formation (Tremadocian, Ordovician), which outcrops to the south of the salar, is composed of alternating sequences dominated by sandstone (Blasco et al. 1996). The Ojo de Colorados Basic Complex, also Ordovician in age, includes stratified gabbros and serpentinites. These medium- to coarse-grained tabular gabbros are interbedded with the Tolillar Formation and exhibit contact metamorphism at their margins (Zappettini et al. 1994, Hongn and Seggiaro 2001).

The upper Eocene Gestes Formation is composed of pale-red polymictic conglomerates containing volcanic and granitic clasts, interbedded with sandstones, representing alluvial fan facies (Pascual 1983, Zappettini et al. 2001). The Pozuelos Formation, ranging from the middle–upper Eocene to the upper Miocene, is subdivided into two members: a lower unit comprising fine to coarse quartz wackes, gypsum, red

claystones, siltstones, and minor conglomerates and eolianites; and an upper unit characterized by claystones, siltstones, and fine quartz wackes, interbedded with halite layers varying from a few millimeters to 40 meters thick (Blasco et al. 1996). The Sijes Formation, dated to the upper Miocene–lower Pliocene, consists of grayish claystones, siltstones, sandstones, and tuffaceous intercalations, with beds of chemical precipitates indicative of lacustrine environments (Blasco et al. 1996).

The current morphostructural configuration of the Salar de Pocitos is the result of post–Lower Miocene deformation processes, as evidenced by the distribution and preservation of Eocene–Miocene stratigraphic units (Jordan and Mpodozis, 2006). These tectonic events, in combination with climatic variability, have strongly influenced the development of the basin, controlling both sedimentation and paleoenvironmental evolution.

METHODOLOGY

The sedimentological analysis was based on the sampling and detailed description of several cores obtained from four drillholes, reaching an average depth of 350 meters. These drillholes are located from the center of the basin to the edge of the evaporitic body in the southern extremity of the Salar de Pocitos (Fig. 3).

Firstly, a detailed description of the stratigraphic and lithological profiles of each drillhole was conducted, with particular emphasis on facies analysis, sedimentary structures, and other key geological attributes. 107 core samples from the four drillholes were analyzed and described. Thin sections were prepared from selected samples of sandstones, breccias, basement rocks, and some evaporites for petrographic analysis under the microscope. The study focused on identifying and

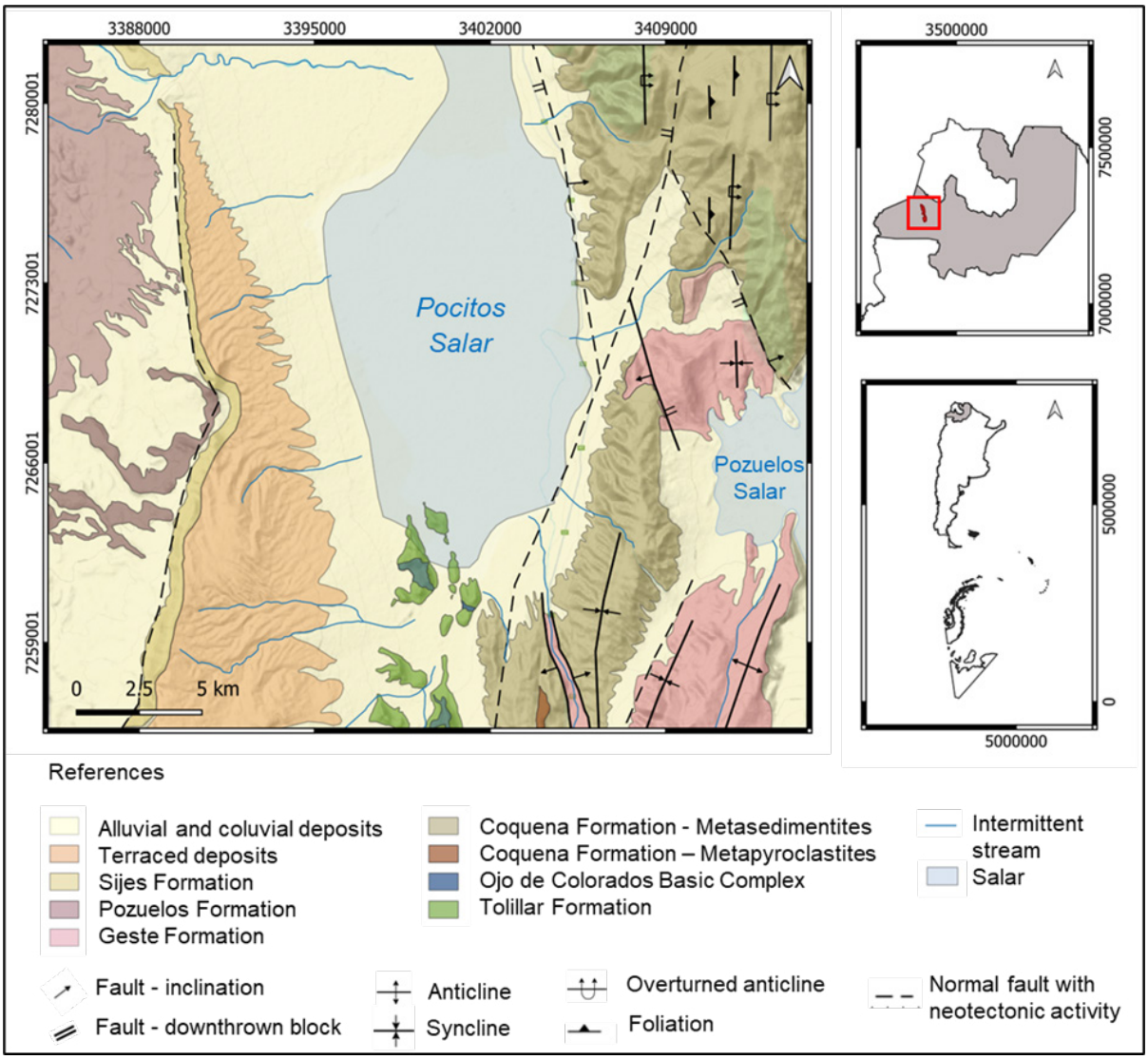

Figure 2. Geological map of the Salar de Pocitos. Modified from Blasco et al. (1996).

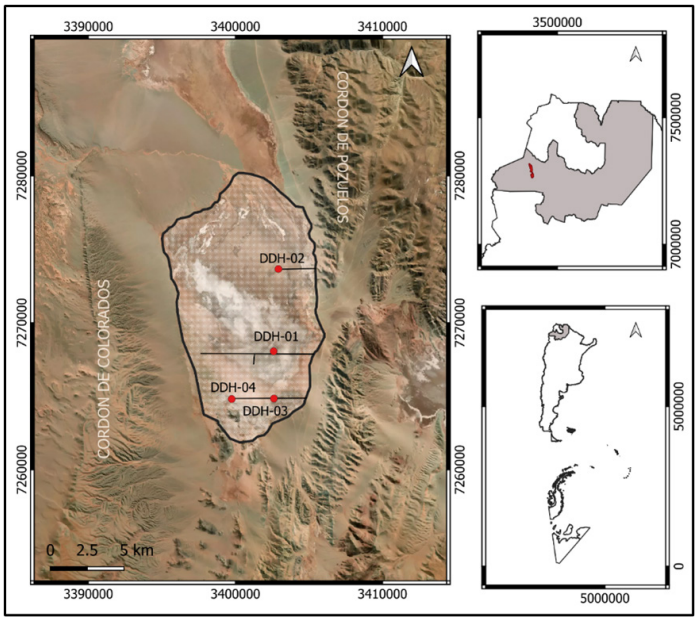

Figure 3. Map of drillhole locations at the southern end of the Salar de Pocitos. EPSG:5345.

describing the primary components and assessing the type and abundance of the matrix. In addition, textural features were characterized by examining primary and accessory minerals, cement types, grain size, shape, roundness, sorting, and grain-to-grain contact types. Diagenetic processes were also evaluated through a quantitative analysis of the rock constituents. The provenance analysis was based on the petrographic examination of 23 sandstone samples obtained from the four drillholes, with the aim of understanding source-to-sink dynamics. Thin sections were prepared from these samples, including 11 from Drillhole 2, seven from Drillhole 3, three from Drillhole 4, and two from Drillhole 1. Quantitative point-counting was conducted on each thin section, with a minimum of 100 grains per sample within the 0.062–2 mm size range. The grains were classified following the scheme of Pettijohn et al. (1973), and the counts were performed using the Gazzi-Dickinson method (Dickinson 1970, Gazzi et al. 1973, Dickinson and Suczek 1979, Dickinson et al. 1983, Ingersoll 1978, Ingersoll and Suczek 1979, Ingersoll et al. 1984).During modal counting, sandstone grain types were classified, and the detrital modes were recalculated to 100% using the Qm–F–Lt and Qt–F–L schemes (Dickinson 1985), as well as the Lm–Lv–Lp proportions. Undulatory quartz grains were interpreted as originating from low-grade metamorphic rocks, while non-undulatory quartz was considered to derive from high-grade metamorphic sources, behaving similarly to plutonic quartz (Basu et al. 1975, Galli et al. 2011). Polycrystalline quartz grains composed of two to five crystals with straight boundaries were classified as plutonic in origin, whereas those with more than five crystals and crenulated contacts were attributed to a gneissic source (Basu et al. 1975). The modal data were subsequently plotted on standard ternary diagrams for tectonic discrimination of detrital sandstones (Dickinson and Suczek 1979, Dickinson et al. 1983, Dickinson 1985).

Based on hand sample observations and petrographic analysis, thirteen sedimentary facies were defined according to lithology, color, texture, and sedimentary structures, which reflect the prevailing physicochemical conditions at the time of deposition. Four Selley-type stratigraphic columns were constructed at a scale of 1:3000. These columns were used to establish a southwest–northeast correlation among the drillholes, allowing the identification of depositional environments and sub-environments, and enabling a detailed characterization of and areal distribution of sedimentary facies allowing the understanding of the evolution across the Salar de Pocitos basin by using Walther´s law.

RESULTS

Core analysis

The sedimentary succession unconformably overlies basement rocks. This basement is highly fractured, and its composition varies with depth. In the southwestern edge of the basin, at a depth of 230 meters, the basement comprises gabbro. Under the petrographic microscope, large crystals of clinopyroxene, plagioclase, and olivine with an ophitic texture, and calcite-filled veins are observed. At greater depths, 320 meters, metacherts with calcite-filled veins are found. In the southeastern edge, the basement is represented by phyllites, low-grade metamorphic rocks with mineral orientation and quartz, calcite, and oxide-filled veins.

Facies Description

Gmm – *Massive matrix-supported breccias:*

This facies consists of disaggregated, brown-colored breccias supported by a fine sand matrix comprising ~40% of the rock. The clasts are poorly sorted and include fragments of basement rocks, quartz, lithic fragments, halite, and gypsum crystals. Clasts are angular to prismatic, ranging from 1 to 36 cm, and are heterogeneously distributed. Cement is carbonate. Beds are 25 cm to 3.8 m thick, with sharp, non-erosive basal contacts (Fig. 4a).

Interpretation: Indicative of high-strength debris flow deposition (Miall 2006).

Gcm – *Massive clast-supported breccias:*

Composed of brown-colored breccias with clasts ranging

from 1 to 7 cm, occasionally exceeding 10 cm. The matrix (15–20%) is sandy-clayey. Clasts are angular and moderately sorted. Beds are 30 cm to 2.2 m thick, with straight basal contacts and carbonate cement (Fig. 4b).

Interpretation: Low-energy, pseudoplastic debris flows resulting from viscous or turbulent transport (Miall 2006).

Sm – *Massive sandstones:*

Fine to medium sandstones with yellowish, reddish, and dark brown hues. The matrix is pelitic; grains are sub-rounded, moderately sorted, with carbonate cement. Some layers contain halite and mirabilite. Bed thicknesses range from 6 cm to 1.29 m, with transitional to sharp contacts (Fig. 4c).

Interpretation: Likely formed from rapid deposition by sediment gravity flows, or modified post-depositionally (e.g., by dehydration or bioturbation) (Miall 2006).

Smy – *Gypsum-rich massive sandstone:*

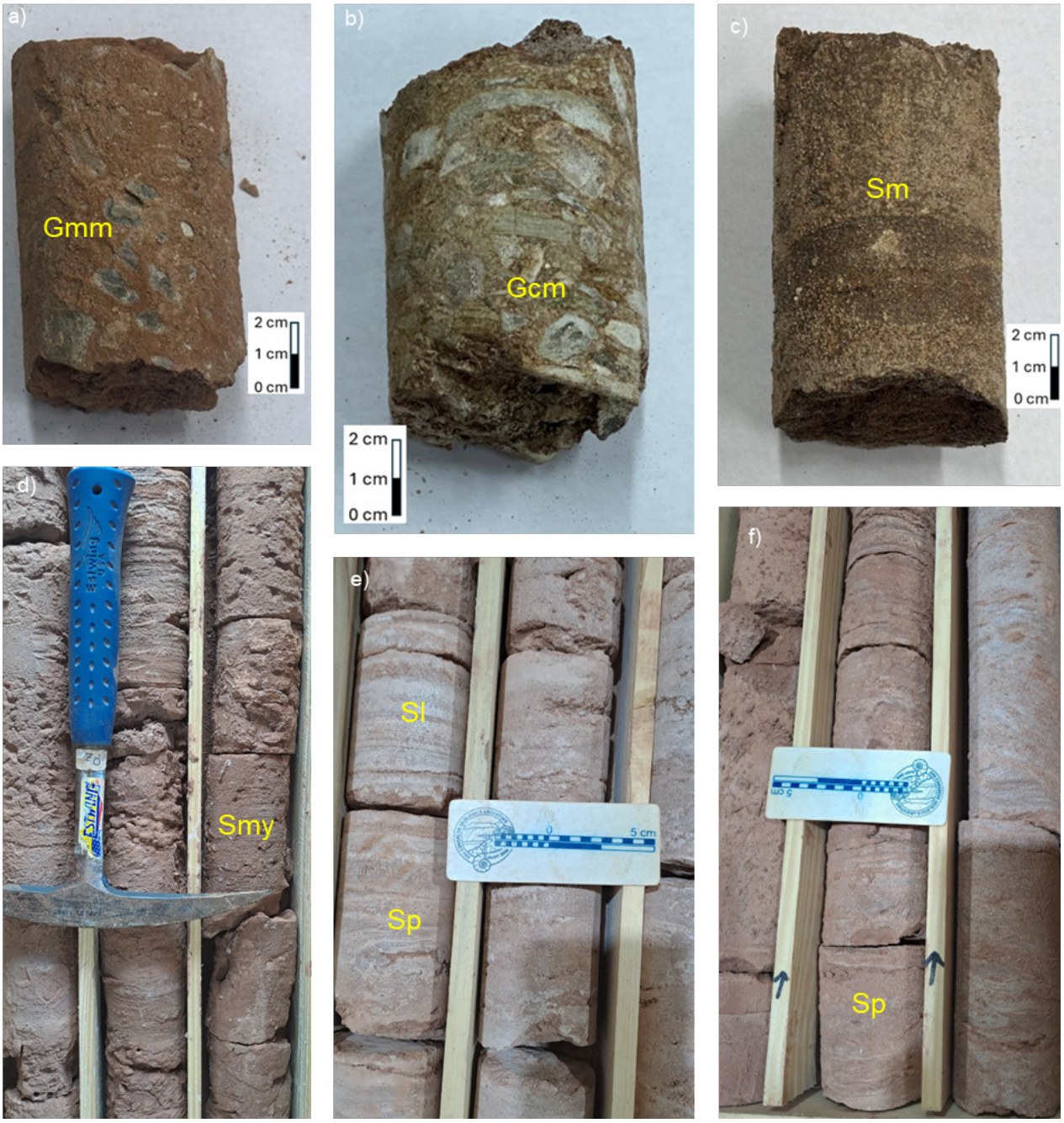

Figure 4. Core sample showing various facies. a) Gmm facies with angular clasts heterogeneously distributed in a sandy matrix; note the poor sorting of the clasts, b) Gcm facies, clast-supported, showing angular clasts and poor sorting, c) Medium sandstone facies (Sm), displaying a dark brownish color and massive structure, d) Smy facies, showing a massive structure and small halite and gypsum crystals in the matrix, e) Sandy facies (Sl) with well-defined parallel lamination alternating with Sp facies, f) Sandy facies with planar cross-bedding (Sp).

Fine to medium brown sandstones containing gypsum microcrystals. Matrix is pelitic with sub-rounded grains, moderate sorting, and carbonate cement. Beds are 5–50 cm thick, with transitional contacts (Fig. 4d).

Interpretation: Formed under hypersaline conditions with intense evaporation, promoting seasonal gypsum crystallization at the sediment-water or sediment-air interface (Ortí Cabo 2010).

Sl – *Laminated sandstone:*

Light yellow, medium-grained sandstones with very fine parallel lamination, silty matrix, and carbonate cement. Moderately sorted, with minor halite content. Beds are 10–60 cm thick, with transitional contacts (Fig. 4e).

Interpretation: Deposits from fluvial channels under subcritical to supercritical flow, typically during high-energy flood events (Miall 2006).

Sp – *Planar cross-bedded sandstone:*

Yellowish, medium-grained sandstone with a clayey matrix and planar cross-bedding. Contains some halite. Beds are 40–70 cm thick with straight contacts (Fig. 4f).

Interpretation: Formed by the migration of 2D dunes in moderate to high-energy fluvial channels, typical of braided or meandering river systems (Miall 2006).

Sfl – *Flaser-bedded sandstone:*

Brown, fine-grained sandstone with a clayey matrix and flaser bedding. No HCl reaction. Beds are 5–10 cm thick, with transitional contacts (Fig. 5g).

Interpretation: Reflects alternating high- and low-energy conditions, typical of fluvial systems with variable discharge, suggesting cyclical flow dynamics (Miall 2006).

Fm – *Massive mudstone:*

Brown-colored massive shales with carbonate cement, sometimes containing dispersed gypsum microcrystals. Beds are 3–67 cm thick with straight contacts (Fig. 5h).

Interpretation: Indicates suspension-dominated deposition during flood events, followed by evaporation under hypersaline conditions (Miall 2006).

Tr – *Banded travertine:*

White travertine with greenish alteration. Beds are 15–80 cm thick with transitional contacts (Fig. 5i).

Interpretation: Formed under saturated presumable hydrothermal subaerial environments with active stream flow and under steep gradients, where CO_2 degassing and biological activity promote carbonate precipitation (Della Porta 2015).

Mb – *Mirabilite-rich facies:*

White, silky-luster mirabilite layers, easily disaggregated. Beds are 0.4–6 cm thick with sharp contacts (Fig. 5j).

Interpretation: Reflects evaporitic environments with Na_2SO_4-rich waters, often derived from granite weathering, high evaporation, and thermal amplitude with seasonal freezing (Ortí Cabo 2010).

Hxx – *Massive halite:*

Cubic, crystalline halite in white and pink hues, with crystal sizes from 0.5 to 2 cm. Beds are 45 cm to 3.37 m thick, with both sharp and transitional contacts (Fig. 5k).

Interpretation: Formed under weak saturation and slow evaporation, producing large, well-formed crystals (Ortí Cabo 2010).

Hxm – *Mud-rich halite:*

Brown halite facies with an arguillaceous-silty to fine sandy

Table 1: Definition of Sedimentary Facies

Facies code	Description	Interpretation
Gmm	Massive breccias matrix support	High energy debris Flow deposits
Gcm	Massive breccias clast support	Low energy pseudoplastic debris flow deposits
Sm	Fine to medium massive sandstone	High energy sediment gravity flows
Smy	Fine to medium massive sandstone, containing gypsum microcrystals	Rapid and continuous sedimentation in a high salinity environment and intense evaporation
Sl	Medium sandstone with fine parallel lamination	Represents fluvial channel deposits under subcritical to supercritical flow conditions
Sp	Medium sandstone with planar cross-stratification	Formed by the migration of two-dimensional dunes
Sfl	Fine sandstone with flasher-type stratification	Variable and Dynamic current regime
Fm	Massive pelite	Conditions where deposition is dominated by fine material transported in suspension during floods or flood events
Tr	Travertines	Interaction of physicochemical and biological processes linked to dynamic fluvial systems
Mb	Mirabilite	Periods of evaporation and freezing
Hxx	Massive cubic crystalline halite	Weak saturations and slow crystallizations
Hxm	Muddy interstitial crystalline halite	Formations of very shallow origin, with influx of detrital material into the crystalline structure
Tb	Tuff	Intermittent volcanic eruptions

Figure 5. Core sample showing various facies. g) Sandstone facies with flaser structures (Sfl), thin pelitic laminae (brown) can be distinguished within the sandy matrix (whitish), h) Core fragment with pelitic facies (Fm), the fracture shows a massive structure and absence of lamination, i) Travertine facies (Tr), is observed the whitish color with well-defined parallel lamination, j) Disintegrated Mb facies, represented by white crystals and silky luster in Fm facies, k) Crystalline halite facies (Hxx), displaying a pink and brown color with massive structure, l) Fragments of muddy halite facies (Hxm), is observed the pelitic matrix, m) Sample of disintegrated volcanic material (Tb).

matrix, showing massive or banded texture. Beds are 7 cm to 2.5 m thick with transitional contacts (Fig. 5l).

Interpretation: Represents very shallow water environments with detrital influx. Suggests subaerial exposure and halite recrystallization (Dumas 1988).

Tb – *Tuff:*

Gray, fine to medium-grained tuff containing small biotite crystals. Beds are 9–34 cm thick, with sharp contacts (Fig. 5m).

Interpretation: Indicates episodic pyroclastic deposition from multiple volcanic events.

Wells stratigraphic successions and correlation

The depocenter in the southern sector of the salar (well one, Fig. 6) is characterized by a complex succession of lithological units, reflecting a dynamic depositional history. At the base, a 45-meter-thick coarsening-upward sequence comprises clast-supported breccias transitioning to matrix-supported breccias. Above this, 78 meters of interfingering fine- to medium-grained sandstones display features such as parallel lamination and flaser structures. These sandstones are interbedded with travertine deposits and a distinct tuff layer. The upper part of the succession features 115 meters of interbedded crystalline halite and fine- to medium-grained sandstones, with abundant gypsum crystals. Another tuff layer appears near the top. The column culminates with 89 meters of interbedded claystone, siltstone, and halite, capped by sulfate-rich layers.

The northern drillhole (well two, Fig. 6) reveals, from bottom to top, 75 meters of coarse sandstones with a basal tuff layer, followed by a 2-meter-thick breccia bed and fine

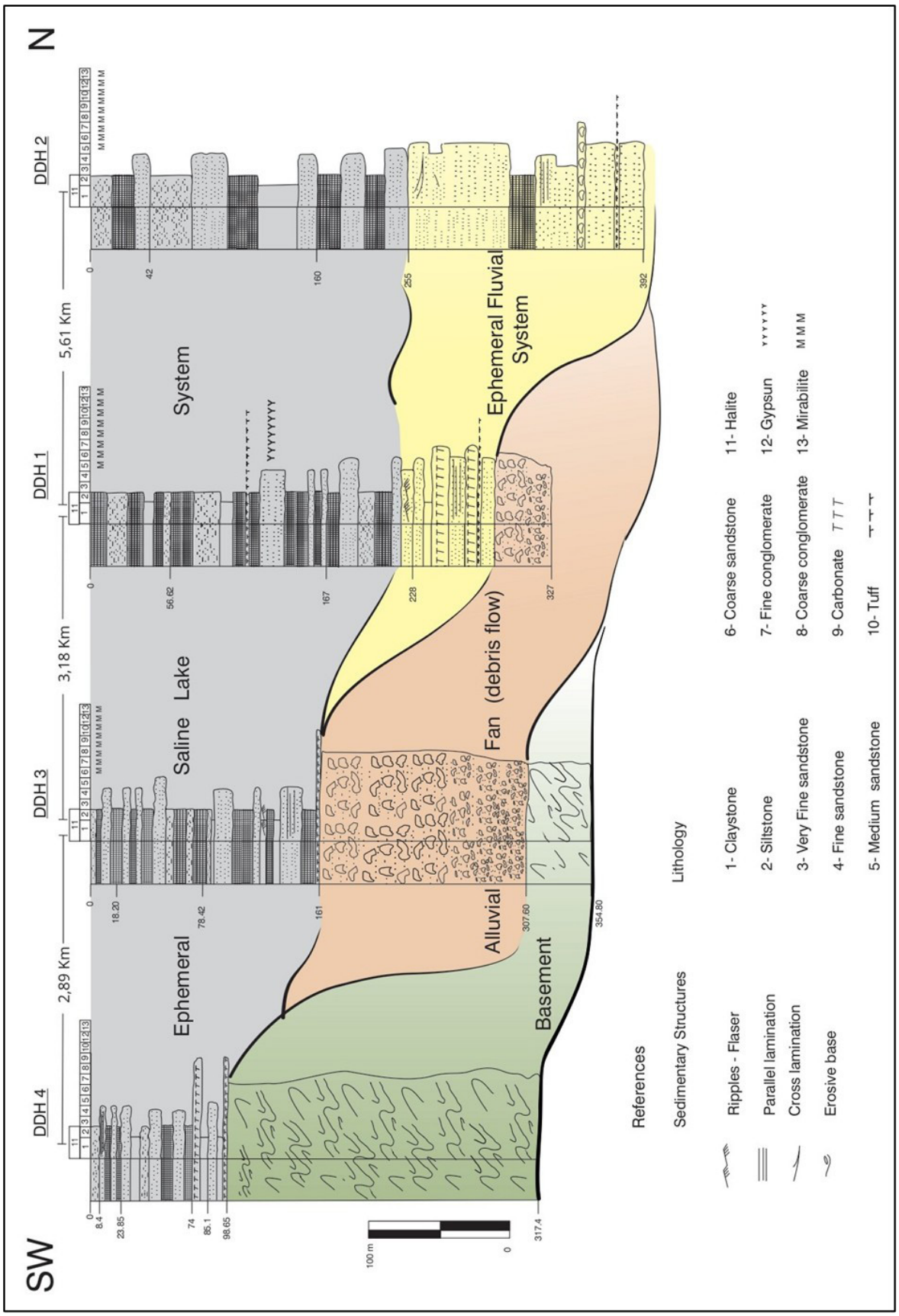

Figure 6. Stratigraphic successions and lateral correlation of the four drillholes analyzed in the southern sector of the Salar de Pocitos.

sandstones with parallel lamination. This is overlain by 15 meters of crystalline halite. Above lies 72 meters of brown and reddish medium-grained sandstones with a clay matrix and tangential lamination, containing minor halite. The upper section consists of 78 meters of massive fine sandstones interbedded with crystalline halite, and finally, 152 meters of alternating claystone, siltstone, crystalline halite, and clay-matrix fine sandstones. The succession ends with limonite deposits containing mirabilite-thenardite.

In the southeastern sector (well three, Fig. 6), the sequence begins with 47.2 meters of basement, overlain by 146.6 meters of coarsening-upward breccias. These transition from clast-supported to matrix-supported breccias with sandy-clay matrices. Above this, a 3-meter-thick travertine layer is followed by 79 meters of interfingering medium- to fine-grained sandstones (with lamination and flaser structures), claystones, and crystalline halite. The uppermost unit comprises 80 meters of massive coarse- to fine-grained sandstones, crystalline halite, and siltstone, with sulphates at the top.

In the southwestern sector (well four, Fig. 6), the basal rocks consist of Ordovician metasedimentary units and serpentinitized gabbro-diorites with carbonate, halite, and sulfate-filled fractures. Above, a 25-meter succession of medium-grained sandstones interbedded with travertines and claystones is followed by 63 meters of crystalline halite, fine- to medium-grained sandstones, claystones, and massive siltstones. Around 10 meters depth, fine sandstones with parallel lamination are identified. The succession concludes with siltstones containing mirabilite-thenardite.

Key stratigraphic markers and distinct facies allowed for lateral correlation among the drillholes (Fig. 6), facilitating the interpretation of spatial facies variability and depositional environments across the basin. It can also be interpreted from the correlation, based on the grain-size fining-and thinning upward arrangement, a long-term backward-stepping pattern, indicating a tectonically-driven accommodation cycle for the basin fill.

Paleoenvironmental analysis and depositional environments

Interpretation is based on facies associations, stratigraphy, sedimentology, and mineralogy from all four drillholes. Three main playa-lake subenvironments are defined: alluvial fan, ephemeral fluvial, and ephemeral saline lacustrine.

Facies association 1 (FA1): Alluvial Fan. Breccias and conglomerates display upward fining trends in the southern salar from clast-supported to matrix-supported types (facies Gmm/Gcm), indicative of debris flow deposits. These facies form in tectonically active zones where relief and accommodation space drive fan evolution (Bull 1977, Allen and Hovius 1998, Ventra and Clarke 2018). Some authors attribute fan formation to climate-driven processes (Harvey et al. 2005). However, the upward coarsening trends within the breccias may reflect episodic depositional pulses linked both to tectonic pulses and climate variability.

Facies association 2 (FA 2): Ephemeral Fluvial System. Fine to coarse sandstones with parallel/tangential lamination, travertine interbeds, and tuff layers define this facies association. Frequent scour surfaces and laminated sandstones (facies Sl, Sp) suggest episodic high-energy flows (Miall 2006). Interbedded evaporites (facies Smy) support deposition under arid/semi-arid climates with seasonal discharge variability (Priddy and Clarke 2020). The association suggests rapid sedimentation during intense precipitation events, typical of the Puna region.

Facies association 3 (FA 3): Ephemeral Saline Lacustrine System. Crystalline halite (Hxx, Hxm), mudstones, and siltstones with sulfates and gypsum crystals (facies Fm) characterize ephemeral saline lakes. These form via surface runoff during infrequent storms and subsequent evaporation-driven brine concentration (Hardie et al. 1978). The cycle leads to laminated evaporite-mudstone sequences. Brine chemistry in the Salar de Pocitos favors gypsum and mirabilite precipitation. These deposits are critical for paleoenvironmental reconstructions and hold economic value, particularly for lithium.

Playa lakes develop where evaporation exceeds inflow, shaped by both climate and tectonics. They are transitional systems, neither consistently wet nor dry (Briere 2000). Tectonics may produce orographic deserts beyond subtropical arid zones, influencing playa distribution (Hardie et al. 1978). The alternation of clastic and evaporitic layers, travertines, and tuffs in the Salar de Pocitos reflects episodic tectonic, volcanic, and climatic influences. These features underscore the basin's complex sedimentological history and potential for economically significant mineral resources.

The stratigraphic succession documented in the Salar de Pocitos, characterized by alternating clastic and evaporitic deposits, reflects the dynamic interplay of depositional processes in this environment. Episodes of tectonic activity, periodic flooding, and intense evaporation are the primary drivers of sedimentation and stacking patterns. The presence of interbedded travertines and volcanic tuffs within this succession further suggests episodic volcanic activity and chemical precipitation, adding complexity to the depositional history, which is punctuated with volcaniclastic events and

Well	2														3						4			1	
Sample	3	5	6	11	12	14	15	16	17	20	23	30	32	38	39	40	45	47	75	76	79	82	85
Monocrystalline quartz (Qm)	47,00	45,00	44,00	52,08	43,20	46,00	50,50	44,45	29,10	20,00	23,47	58,40	56,38	51,50	49,30	53,00	56,00	62,00	45,00	47,66	39,99	43,00	51,30
Monocrystalline quartz with undulatory extinction	2,50	2,00	4,20	3,02	5,90	6,00	7,00	10,00	13,20	8,90	10,00	2,60	0,00	7,70	6,20	1,30	2,80	0,00	3,00	0,00	6,00	3,20	2,00
Quartz in plutonic rock	10,30	20,00	11,00	4,98	12,00	16,00	6,48	2,54	11,60	0,00	0,00	18,30	12,62	20,00	17,00	11,20	10,60	12,00	20,00	11,34	18,02	12,00	16,00
Quartz in metamorphic rock	2,78	3,40	2,64	0,00	0,00	0,00	0,00	8,00	0,00	11,06	4,52	3,50	3,00	3,80	2,20	3,78	4,00	1,30	4,00	6,00	0,00	3,00	4,10
Chert	2,40	3,60	0,00	0,00	0,00	0,00	3,75	0,00	2,50	0,00	0,00	0,00	0,00	0,00	0,00	2,00	1,00	0,00	0,00	2,00	0,00	2,50	0,00
Potassium feldspar (FK)	6,70	8,00	1,86	13,02	9,70	19,20	2,45	7,11	14,40	7,71	8,83	7,20	1,70	10,73	4,80	6,00	5,50	8,00	19,25	12,60	9,66	3,60	5,00
Plagioclase	23,60	15,00	28,30	21,90	23,30	4,80	24,54	24,90	19,30	22,28	29,17	4,00	21,30	6,27	16,50	17,72	16,10	8,70	8,75	9,20	19,33	25,70	18,70
Volcanic lithics	0,00	0,00	0,00	0,00	0,00	0,00	0,00	0,00	1,50	0,00	0,00	0,00	0,00	0,00	0,00	0,00	0,00	0,00	0,00	0,00	0,00	0,00	0,00
Metamorphic lithics	0,00	1,00	2,00	0,00	0,00	0,00	0,00	1,50	3,00	5,00	6,23	2,00	2,00	0,00	0,00	0,00	1,00	2,00	0,00	3,00	2,00	3,00	0,00
Sedimentary lithics	4,72	2,00	6,00	2,00	5,90	8,00	5,28	1,50	5,40	25,05	17,78	4,00	3,00	0,00	4,00	5,00	3,00	6,00	0,00	8,20	5,00	4,00	2,90
Micas	0,00	0,00	0,00	3,00	0,00	0,00	0,00	0,00	0,00	0,00	0,00	0,00	0,00	0,00	0,00	0,00	0,00	0,00	0,00		0,00	0,00	0,00
Total	100,00	100,00	100,00	100,00	100,00	100,00	100,00	100,00	100,00	100,00	100,00	100,00	100,00	100,00	100,00	100,00	100,00	100,00	100,00	100,00	100,00	100,00	100,00
Qt	64,98	74,00	61,84	61,90	61,10	68,00	67,73	64,99	56,40	39,96	37,99	82,80	72,00	83,00	74,70	71,28	74,40	75,30	72,00	67,00	64,01	63,70	73,40
F	30,30	23,00	30,16	36,00	33,00	24,00	26,99	32,01	33,70	29,99	38,00	11,20	23,00	17,00	21,30	23,72	21,60	16,70	28,00	21,80	28,99	29,30	23,70
L	4,72	3,00	8,00	2,10	5,90	8,00	5,28	3,00	9,90	30,05	24,01	6,00	5,00	0,00	4,00	5,00	4,00	8,00	0,00	11,20	7,00	7,00	2,90
Qm	49,50	47,00	48,20	56,74	49,10	52,00	57,50	54,45	42,30	28,90	33,47	61,00	56,38	59,20	55,50	54,30	58,80	62,00	48,00	47,66	45,99	46,20	53,30
F	30,30	23,00	30,16	35,97	33,00	24,00	26,99	32,01	33,70	29,99	38,00	11,20	23,00	17,00	21,30	23,72	21,60	16,70	28,00	21,80	28,99	29,30	23,70
Lt	20,20	30,00	21,64	7,29	17,90	24,00	15,51	13,54	24,00	41,11	28,53	27,80	20,62	23,80	23,20	21,98	19,60	21,30	24,00	30,54	25,02	24,50	23,00
Lm	21,25	18,00	29,66	0,00	0,00	0,00	0,00	78,90	18,63	100,00	100,00	23,10	28,37	15,96	11,45	25,23	34,24	21,56	16,66	44,24	10,00	33,30	20,40
Lv	0,00	0,00	0,00	0,00	0,00	0,00	0,00	0,00	9,31	0,00	0,00	0,00	0,00	0,00	0,00	0,00	0,00	0,00	0,00	0,00	0,00	0,00	0,00
Lp	78,74	82,00	70,33	100,00	100,00	100,00	100,00	21,10	72,06	0,00	0,00	76,89	71,62	84,03	88,54	74,76	65,75	78,43	83,33	55,75	90,00	66,60	79,60

Table 2: Composition of sandstone grains recalculated to 100%

hydrothermal inputs. Moreover, this volcanic influence may have significantly affected brine chemistry and the precipitation of specific mineral phases.

From a geological perspective, playa-lake deposits are valuable not only as records of past arid climatic conditions and paleoenvironmental evolution but also for their economic potential. Additionally, these settings often host a variety of rare evaporite minerals and industrially significant elements, such as lithium (Reeves 1978).

Sandstone provenance

Modal analysis data from 23 sandstone samples (Table 2, Fig. 7, Fig. 8) were projected onto ternary diagrams for tectonic discrimination. In the Q-F-L diagram (Fig. 7a), most samples cluster in the quartzose feldspar field. In the Qt-F-L diagram (Fig. 7b), they fall into the continental transition and recycled orogen fields, with one sample from well two in the dissected arc field. The Qm-F-Lt diagram (Fig. 7c) displays sample distribution across continental transition, quartzose recycled orogen, dissected arc, and mixed fields, with the mixed field dominating. The Lm-Lv-Lp diagram (Fig. 7d) suggests a predominant plutonic origin with minor metamorphic contributions, while the Lm-Ls-Lp diagram (Fig. 7e) points to sedimentary provenance.

Petrographic characteristics, particularly from the depocenter and northern area (Fig. 8), indicate continental transition source areas composed of medium- to high-grade metamorphic rocks. This is evidenced by high Qm/Qp ratios and low FK/P values (Dickinson 1985). Some samples also fall within the quartzose recycled orogen zone (Qm > Lt), indicating sources with multiple erosion-deposition cycles from surrounding reactivated mountain belts.

The mixed field dominance implies tectonic and climatic influences blending materials from various sources. Samples

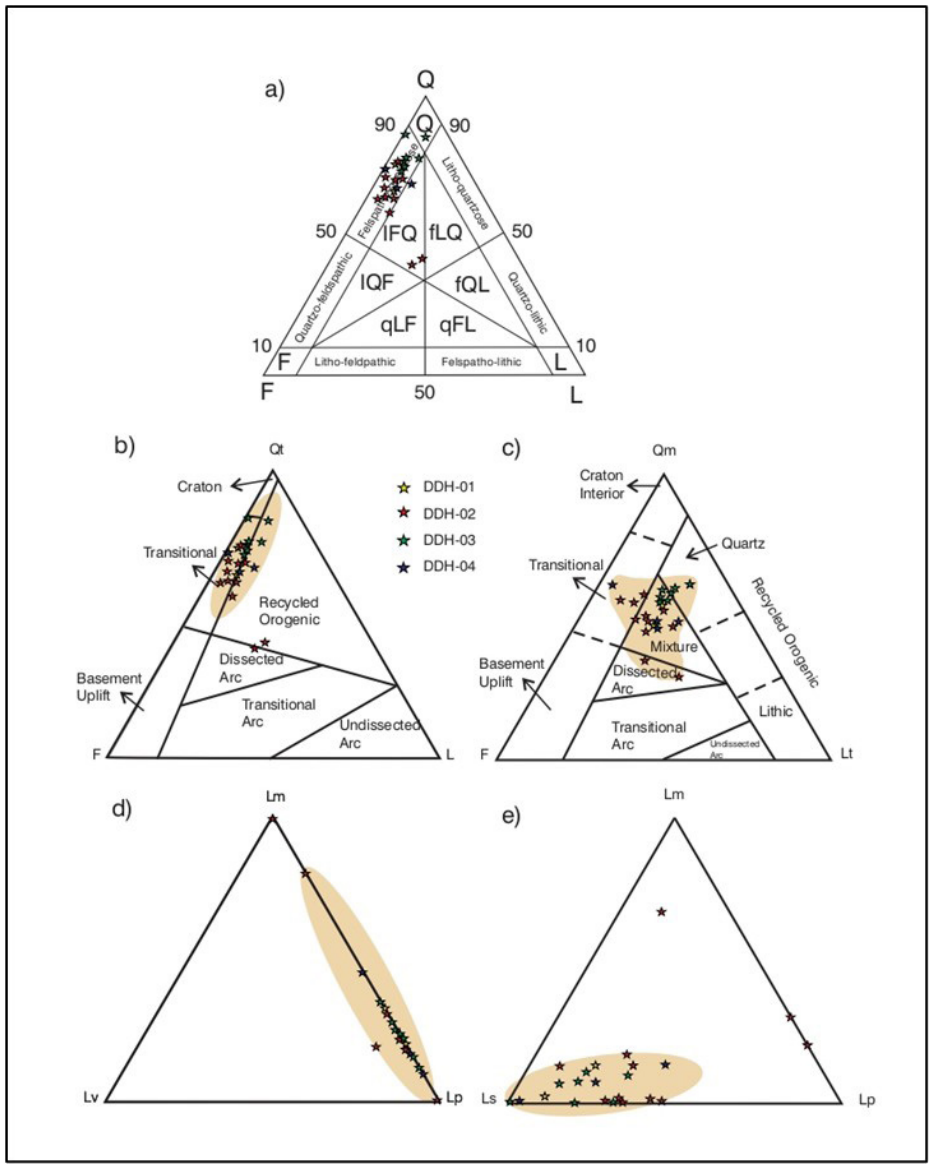

Figure 7. QtFL, QmFLt and LmLvLp provenance discrimination diagrams of the Salar de Pocitos showing: a) Sandstone samples located in the quartz feldspar field b) High concentration in the transition fields and recycled orogen, c) Samples concentrated in the mixed field, d) Sandstone samples concentrated along the edge of metamorphic and plutonic rocks, e) Sandstone samples concentrated in sedimentary lithics.

in the recycled orogen and dissected arc fields suggest contributions from both high-elevation, heavily eroded regions and volcanic terrains (Dickinson and Suczek 1979). The composition of the sandstones is consistent with that of the more proximal clasts in the analyzed breccias and conglomerates, supporting a source-to-sink analysis that indicates proximity to the source areas and the endorheic nature of the dominant drainage systems associated to active border faults. Figure 8 shows representative microphotographs of sandstone grains.

DISCUSSION

Among the sedimentary units identified, several facies show promise as reservoirs for lithium-rich brines. These include fine- to coarse-grained sandstones with moderate sorting (Sm, Smy, Sl). In the depocenter and northern sector (wells one and two), these facies range in thickness from 5 cm to 1.3 m, are found at depths between 30 and 120 m, and demonstrate sufficient lateral continuity for reservoir development. Additionally, these intervals are frequently interbedded with sealing facies such as halite (Hxx) and claystone (Fm), enhancing their reservoir potential.

The depositional patterns observed in the southern sector of the Salar de Pocitos—especially the alternation of clastic and evaporitic facies—bear strong resemblance to other endorheic basins of the Central Andes, such as the Salar de Pastos Grandes (Alonso 1992) and the Salar del Hombre Muerto (Vinante and Alonso 2006). At Pastos Grandes, the Cenozoic stratigraphic succession records an alternation of fluvial, lacustrine, and evaporitic deposits (Alonso 1992), influenced by tectonic subsidence and climatic fluctuations that control lake levels and salinity. The presence of borate-rich layers in the Sijes Formation, interbedded with siliciclastic and volcanic deposits, mirrors the sedimentary patterns seen in Pocitos, especially the interplay among sandstones, claystones, and evaporites.

These similarities highlight the regional role of volcanism, climatic cycles, and tectonics in shaping facies distribution and stratigraphic architecture, largely influenced by active accommodation as the main controlling factor of Puna subbasins. Within this setting dominant lacustrine playa-lakes with evaporites laterally linked to alluvial fans give rise to characteristic evaporite facies models reflecting underfilled lake basins with persistently closed hydrology (cf. Caroll and Bohacs 1999, Bohacs et al. 2000). Similarly, at Hombre Muerto, Vinante and Alonso (2006) described a lateral facies zonation from marginal clastic-carbonate deposits to borate- and halite-rich depocenters. This pattern, shaped by hydrology and primary topographic gradientes, resembles the facies organization in Pocitos, where alluvial and fluvial clastics transition (physically interfinger) into evaporitic lacustrine facies better preserved toward the central and northern sectors. These analogies reinforce the predictive potential of facies distribution in endorheic systems, which is essential

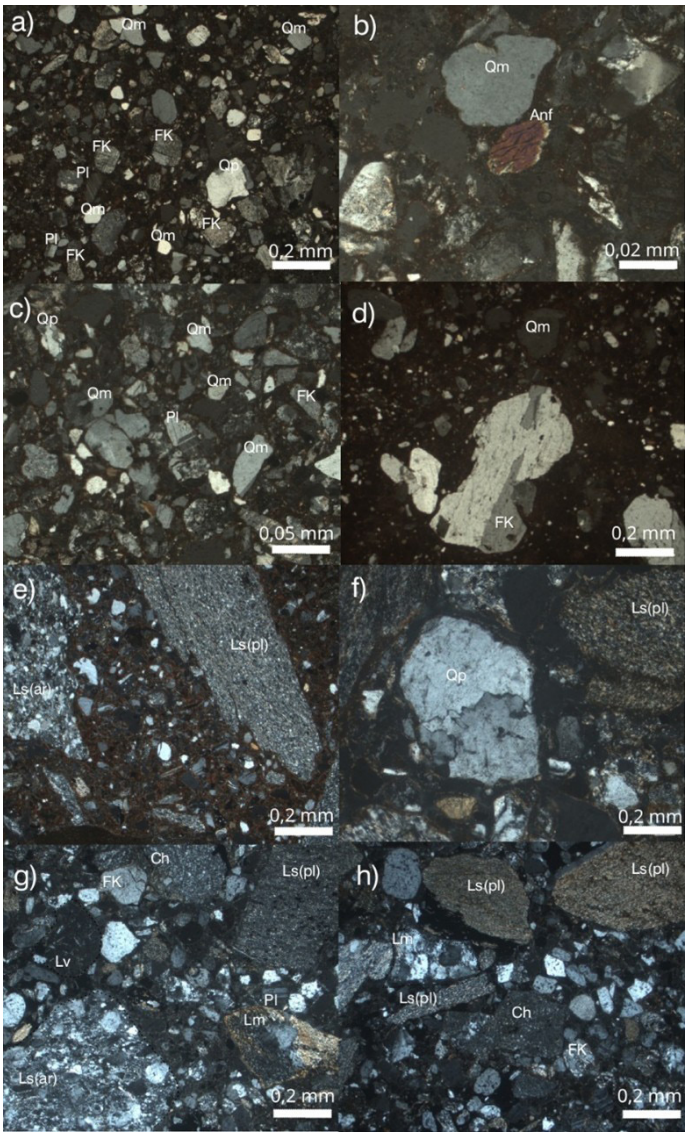

Figure 8. Photomicrographs of sandstone samples under cross-polarized light. a) Sandstone sample with abundant rounded monocrystalline quartz grains (Qm), potassium feldspar (FK) and plagioclase (Pl). The matrix is composed of fine material and is abundant, b) Subrounded monocrystalline quartz grain (Qm). The presence of an amphibole grain (Anf) in the basal section is highlighted, c) Photomicrograph showing a predominance of rounded to sub-rounded monocrystalline quartz (Qm) with plagioclase (Pl) and potassium feldspar (FK) in a clayey matrix, d) A potassium feldspar (FK) phenocrystal is observed, e) Angular to subangular sedimentary lithic fragments (Ls), of different sizes, including pelites (pl) and sandstones (ar), f) Polycrystalline quartz grain (Qp) with saturated contacts, g) Sandstone with poor sorting and abundance of sedimentary lithic fragments (Ls pl and ar), volcanic (Lv) and metamorphic (Lm), h) Photomicrograph showing a predominance of lithic fragments, chert (Ch) and potassium feldspar (KF) with angular to subangular clasts and poor sorting.

for resource evaluation and modeling. Nevertheless, notable differences exist in methodology and basin fill geochemistry. Studies in Hombre Muerto and Pastos Grandes primarily rely on surface mapping and shallow wells, whereas this study draws from over 100 core samples and detailed petrographic analyses across four drillholes. This subsurface approach enables more accurate vertical facies characterization and direct well-to-well correlation, offering a deeper understanding of sedimentary patterns and basin architecture. Additionally, while Pastos Grandes and Hombre Muerto feature borate-rich layers (notably ulexite), indicative of boron-rich hydrochemical systems influenced by altered pyroclastics and hydrothermal fluids, no borates were observed in Pocitos. Instead, evaporites here are dominated by halite and sulfates, reflecting a distinct geochemical evolution and solute source.

A limitation of this study is the absence of absolute dating, which constrains the establishment of a precise depositional chronology. Nonetheless, sedimentological attributes and facies correlations support a coherent interpretation of basin evolution. Detailed core descriptions, thin section analyses, facies classification, and sandstone provenance studies together provide critical insights into depositional dynamics and paleoenvironmental conditions. Future work should include radiometric dating (e.g., biotite from tuff layers) to refine the temporal framework. Additionally, comprehensive mineralogical analyses of clays and evaporites—currently underway—will further elucidate diagenetic processes and chemical environments, strengthening sedimentological interpretations and understanding of post-depositional evolution in the salar.

CONCLUSIONS

Facies analysis, stratigraphic columns, and well correlations identify three main subenvironments in the southern sector of the Salar de Pocitos: alluvial fan, ephemeral fluvial, and ephemeral lacustrine systems. These subenvironments together constitute a lacustrine playa-lake alluvial fan evaporite setting consistent with continental evaporite facies models typical of high accommodation settings and underfilled lake development with persistently closed hydrology. Sandstone provenance analysis reveals contributions from multiple tectonic sources. The predominance of continental transition and recycled orogen signatures, combined with volcanic input from dissected arcs, indicates a complex erosional history involving tectonic uplift and exhumation of metamorphic and igneous source areas. Sandstone petrography enabled a source-to-sink analysis, revealing recycled orogen and continental transition signatures likely derived from the Coquena Formation, located east of the Salar de Pocitos. This Ordovician unit consists of metasedimentary, metapyroclastic, metavolcanic, and sedimentary rocks and is marked by intense faulting and neotectonic activity (Jordan and Mpodozis 2006, Hongn et al. 2010). In contrast, samples with dissected arc characteristics likely originate from the Ojo de Colorados Basic Complex to the south, comprising gabbroic and dioritic rocks, some of which are serpentinized. The Salar de Pocitos basin is rich in sulfates, as indicated by the presence of minerals such as gypsum, mirabilite, and thenardite.

The sedimentary fill in the southern Salar de Pocitos reflects a dynamic depositional history governed by tectonic activity, alternating climatic conditions, and sedimentological processes. These factors created a mosaic of subenvironments within the broader playa-lake system.

This study advances the understanding of the Puna salars by providing new insights into the sedimentary evolution and paleoenvironmental conditions of the Salar de Pocitos. The findings not only contribute to regional geological models but also inform the exploration and sustainable development of mineral resources—particularly lithium—within the basin.

ACKNOWLEDGMENTS

The authors are grateful to Litica Resources S.A. for providing the core samples and thin sections necessary for this study, and to the Agencia Nacional de Promoción de la Investigación, el Desarrollo Tecnológico y la Innovación for funding this research, which was fundamental to the development of this work. We acknowledge the careful reviews and the editorial management of the manuscript that significantly improve our work. Special acknowledgements to the Editor in chief Ricardo Astini that carefully reviewed the final English version.

REFERENCES

Allen, P.A. and Hovius, N. 1998. Sediment supply from landslide-dominated catchments; implications for basin-margin fans. Basin Research 10: 19–35.

Alonso, R.N. 2006. Ambientes Evaporíticos Continentales de Argentina. INSUGEO, Serie Correlación Geológica 21: 155-170.

Alonso, R. N. 1992. Estratigrafía del Cenozoico de la cuenca de Pastos Grandes (Puna Salteña) con énfasis en la Formación Sijes y sus boratos. Revista de la Asociación Geológica Argentina 47(2): 189-199.

Alonso, R., Viramonte, J., and Gutiérrez, R. 1984. Puna Austral. Bases para el subprovincialismo geológico de la Puna Argentina. 9° Congreso Geológico Argentino, Actas 1:43-63. San Carlos de Bariloche.

Basu, S.W., Young, L.J., Suttner, J.C., and Mack, G.H. 1975. Re-evaluation of the use of ondulatory extinction and polycrystallinity in detrital quartz for provenance interpretation. Journal of Sedimentary Petrology 45(4): 873 -882.

Battaglia, R.R., Sánchez, M.C., Esteban, J., and Salfity, J. A. 2001. Las facies evaporíticas en el salar de Pocitos, Puna de Salta. 7° Congreso Argentino de Geología Económica, Actas 2: 61-62, Salta.

Bohacs, K.M., Carroll, A.R. Neal, J.E., and Mankiewicz, P.J., 2000. Lake-basin type, source potential, and hydrocarbon character: an integrated-sequence-stratigraphic–geochemical framework, in: Gierlowski-Kordesch, E.H. and Kelts, K.R. (eds.), Lake basins through space and time. American Association of Petroleum Geologists. Studies in Geology, 46: 3–34.

Blasco, G., Zappettini, E., and Hong, F. 1996. Hoja Geológica 2566-I San Antonio de los Cobres. Provincias de Salta y Jujuy. Subsecretaría de Minería de la Nación. Dirección Nacional del Servicio Geológico. 126 p., Buenos Aires.

Briere, P. R. 2000. Playa, lago playa, sabkha: Definiciones propuestas para términos antiguos. Journal of Arid Environments 45(1): 1-7.

Bull, W. B. 1977. The alluvial-fan environment. Progress in Physical Geography 1(2): 222–270.

Carroll, A.R., and Bohacs, K.M. 1999. Stratigraphic classification of ancient lakes: balancing tectonic and climatic controls. Geology, 27:99–102.

Della Porta, G. 2015. Carbonate build-ups in lacustrine, hydrothermal and fluvial settings: comparing depositional geometry, fabric types and geochemical signature. Geological Society, 418(1), 17-68, London.

Dickinson, W.R. 1970. Interpreting detrital modes of graywacke and arkose. Journal of Sedimentary Petrology 40(2): 695-707.

Dickinson, W.R. and Suczek, C.A. 1979. Plate tectonics and sandstone compositions, American Association of Petroleum Geologists Bulletin 63: 2164- 2182.

Dickinson, W.R., Beard, L.S., Brakwnringe, G.R., Erjavec, J.L., Ferguson, R.C., Inman, K.F., Knepp, R.A., Lindberg, F.A., and Ryberg, P.T. 1983. Provenances of North American Phanerozoic sandstones in relations to tectonic setting. Geological Society of America Bulletin 94: 222- 235.

Dickinson, W.R. 1985. Interpreting provenances relations from detrital models of sandstone. En Zuffa, G. (ed.) Provenances of arenitas, Reidel Publishing Company, Serie 148: 333- 361.

Dumas, D. 1988. Le Paléogène salifère du bassin de Valence (Sud-Est de la France). Géometrie et sédimentologie des dépôts. Synthèse de bassin. Doctoral dissertation, Thèse Univ. Claude-Bernard, 280 p., Lyon.

Galli, C. I., Ramírez, A., Reynolds, J., Viramonte, J. G., Idleman, B., and Barrientos, C. 2011. Procedencia de los depósitos del Grupo Payogastilla (Cenozoico), río Calchaquí, provincia de Salta. Revista de la Asociación Geológica Argentina 68: 261-276.

Gazzi, P., Zuffa, G.G., Gandolfi, G., and Paganelli, L. 1973. Provenienza e dispersione litoranea delle sabbie delle spiagge adriatiche fra le foci dell'Isonzo e del Foglia: inquadramento regionale: Societa Geologica Italiana, Memorie 12: 1-37.

Gulliford A.R., Flint, S.S., and Hodgson, D.M. 2014. Testing applicability of models of distributive fluvial systems or trunk rivers in ephemeral systems: reconstructing 3-D fluvial architecture in the Beaufort Group, South Africa. Journal of Sedimentary Research 84(12): 1147-1169.

Hardie, L. A., Smoot, J. P., and Eugster, H. P. 1978. Saline lakes and their deposits: A sedimentological approach. Modern and ancient lake sediments, pp.7-41.

Harvey, A.M., Mather, A.E., and Stokes, M. 2005. Alluvial fans: Geomorphology, sedimentology, dynamics - Introduction. A review of alluvial-fan research. Geological Society Special Publication 251: 1–7.

Hongn, F. and Seggiaro, R. 2001. Hoja Geológica 2566-III, Cachi. Programa Nacional de Cartas Geológicas de la República Argentina, Boletin 248: 87 p., Buenos Aires.

Hongn F., Mon R., Petrinovic I., del Papa C., and J. Powell 2010. Inversión y reactivación tectónicas cretácico-cenozoicas en el Noroeste Argentino: Influencia de las heterogeneidades del basamento Neoproterozoico-Paleozoico inferior. Revista de la Asociación Geológica Argentina 66 (1): 38 – 53.

Igarzábal, A.P. 1996. Los salares de la Puna Argentina (provincias de Jujuy, Salta y Catamarca). Instituto de Beneficios de Minerales. Universidad Nacional de Salta (inédito), 120 p., Salta.

Ingersoll, R.V. 1978. Petrofacies and petrologic evolution of the late Cretaceous Fore-arc Basin, Northern and central California. Journal of Geology 86: 335-352.

Ingersoll, R.I., Bullard, T.F., Ford, R.L., Grimm, J.P., Picle, J.D., and Sares, S.W. 1984. The effect of grain size on detrital modes: a test of the Gazzi-Dickinson point-counting method. Journal of Sedimentary Petrology 54(1): 103-116.

Ingersoll, R.V. and Suczek, C.A. 1979. Plate tectonics and sandstone compositions. American Association of Petroleum Geologists Bulletin 63: 2164- 2182.

Jordan, T.E. and Mpodozis, C. 2006. Estratigrafía y evolución tectónica de la cuenca Paleógena Arizaro-Pocitos, Puna Occidental (24-25° S). 11° Congreso Geológico Chileno, Actas 2: 5-60.

Miall, A.D. 2006. The geology of fluvial deposits: Sedimentary facies, basin analysis, and petroleum geology. Springer.

Nichols, G. 2009. Sedimentology and stratigraphy. John Wiley & Sons.

Ortí Cabo, F. 2010. Evaporitas: introducción a la sedimentología evaporítica. In: Arche A. (ed.), Sedimentología, del proceso físico a la cuenca sedimentaria. Consejo Superior de Investigaciones Científicas: 675-756, España.

Pascual, R. 1983. Novedosos marsupiales paleógenos de la Fm. Pozuelos de la Puna, Salta. Ameghiniana 20: 265 - 280. Buenos Aires.

Pettijohn, F., Potter, P.E., and Siever, R. 1973. Sand and Sandstones: Springer Verlag, 618 p., New York.

Priddy, C.L. and Clarke, S. M. 2020. The sedimentology of an ephemeral fluvial–aeolian succession. Sedimentology 67(5): 2392-2425.

Reeves Jr, C.C. 1978. Economic significance of playa lake deposits. Modern and ancient lake sediments 279-290.

Sánchez, M.C., Sastre, V.E., and Salfity, J.A. 2003. Geomorfología de la Cuenca del Salar de Pocitos, Puna Argentina. 2° Congreso Argentino de Cuaternario y Geomorfología, Actas 1: 379-388, Tucumán.

Silva, P., Harvey, A.M., Zazo, C. and Goy, J. 1992. Geomorphology, depositional style and morphometric relationships of Quaternary alluvial fans in the Guadalentin depression (Murcia, southeast Spain). Zeitschrift fur Geomorphologie 36: 325–341.

Turner, J.C.M., 1960. Estratigrafía de la Sierra Santa Victoria y adyacencias. Academia Nacional de Ciencias. Boletín 41(2): 163-196.

Turner, J.C.M. and Méndez, V. 1979. Puna. In Simposio de Geología Regional Argentina. Academia Nacional de Ciencias, 2: 91-116. Córdoba

Ventra, D. and Clarke, L.E. 2018. Geology and geomorphology of alluvial and fluvial fans: Current progress and research perspectives. Geological Society Special Publication 440(1): 1–21.

Vinante, D. and Alonso, R.N. 2006. Evapofacies del salar Hombre Muerto, Puna Argentina: distribución y génesis. Revista de la Asociación Geológica Argentina 61(2): 286-297.

Warren, J.K. 2016. Evaporites: A Geological Compendium. Springer, Second Edition, 1813 pgs. Berlin.

Weissmann, G.S., Hartley, A.J., Nichols, G.J., Scuderi, L.A., Olson, M., Buehler, H., and Banteah, R. 2010. Fluvial form in modern continental sedimentary basins: distributive fluvial systems. Geology 38(1): 39-42.

Whipple, K.X. and Trayler, C.R. 1996. Tectonic control on fan size: the importance of spatially variable subsidence rates. Basin Research 8: 351– 366.

Zappettini, E. O., Blasco, G. and Villar, L.1994. Geología del extremo sur del Salar de Pocitos, Provincia de Salta, República Argentina. 7° Congreso Geológico Chileno, Actas 1: 220-224, Concepción.

Zappettini, E. O., Blasco, G., Ramallo, E. E. and González, O. E. 2001. Hoja Geológica 2569-II, Socompa. Programa Nacional de Cartas Geológicas de la República Argentina, Boletin 260: 53 p., Buenos Aires.